Burns & Trauma, 2023, 11, tkac052
https://doi.org/10.1093/burnst/tkac052
Research Article

OXFORD

Research Article

Skin 11β-hydroxysteroid dehydrogenase type 1 enzyme expression regulates burn wound healing and can be targeted to modify scar characteristics

Kevin H.-Y. Tsai[1,2], Huaikai Shi[2], Roxanne J. Parungao[2], Sina Naficy[3], Xiaotong Ding[4], Xiaofeng Ding[5], Jonathan J. Hew[2], Xiaosuo Wang[6], Wojciech Chrzanowski[7], Gareth G. Lavery[8], Zhe Li[9], Andrea C. Issler-Fisher[9], Jun Chen[4], Qian Tan[5], Peter K. Maitz[2,9], Mark S. Cooper[1,†] and Yiwei Wang[2,4,†,*]

[1]Adrenal Steroid Group, ANZAC Research Institute, Concord Hospital, The University of Sydney, Sydney, NSW 2137, Australia, [2]Burns and Reconstructive Surgery Research Group, ANZAC Research Institute, Concord Hospital, The University of Sydney, Sydney, NSW 2137, Australia, [3]School of Chemical and Biomolecular Engineering, The University of Sydney, Sydney, NSW 2006, Australia, [4]Jiangsu Provincial Engineering Research Centre of TCM External Medication Development and Application, Nanjing University of Chinese Medicine, Nanjing, Jiangsu, 210023, China, [5]Department of Burns and Plastic Surgery, Nanjing Drum Tower Hospital Clinical College, Nanjing University of Chinese Medicine, Nanjing, Jiangsu, 210008, China, [6]Heart Research Institute, The University of Sydney, Sydney, NSW 2006 , Australia, [7]Sydney Nano Institute, Sydney Pharmacy School, Faculty of Medicine and Health, The University of Sydney, Sydney, NSW 2006, Australia, [8]Department of Biosciences, Centre for Healthy Ageing and Understanding Disease, Nottingham Trent University, NG1 4BU, UK and [9]Burns and Reconstructive Surgery Unit, Concord Repatriation General Hospital, Sydney, NSW 2137, Australia

*Correspondence. Email: yi.w.wang@sydney.edu.au; yiweiwang@njucm.edu.cn

[†]These authors contributed equally to this work as the co-senior authors.
Received 26 July 2022; Revised 29 September 2022; Accepted 16 November 2022

Abstract

Background: Excessive scarring and fibrosis are the most severe and common complications of burn injury. Prolonged exposure to high levels of glucocorticoids detrimentally impacts on skin, leading to skin thinning and impaired wound healing. Skin can generate active glucocorticoids locally through expression and activity of the 11β-hydroxysteroid dehydrogenase type 1 enzyme (11β-HSD1). We hypothesised that burn injury would induce 11β-HSD1 expression and local glucocorticoid metabolism, which would have important impacts on wound healing, fibrosis and scarring. We additionally proposed that pharmacological manipulation of this system could improve aspects of post-burn scarring.

Methods: Skin 11β-HSD1 expression in burns patients and mice was examined. The impacts of 11β-HSD1 mediating glucocorticoid metabolism on burn wound healing, scar formation and scar elasticity and quality were additionally examined using a murine 11β-HSD1 genetic knockout model. Slow-release scaffolds containing therapeutic agents, including active and inactive glucocorticoids, were developed and pre-clinically tested in mice with burn injury.

Results: We demonstrate that 11β-HSD1 expression levels increased substantially in both human and mouse skin after burn injury. 11β-HSD1 knockout mice experienced faster wound healing than wild type mice but the healed wounds manifested significantly more collagen deposition, tensile

strength and stiffness, features characteristic of excessive scarring. Application of slow-release prednisone, an inactive glucocorticoid, slowed the initial rate of wound closure but significantly reduced post-burn scarring via reductions in inflammation, myofibroblast generation, collagen production and scar stiffness.

Conclusions: Skin 11β-HSD1 expression is a key regulator of wound healing and scarring after burn injury. Application of an inactive glucocorticoid capable of activation by local 11β-HSD1 in skin slows the initial rate of wound closure but significantlyimproves scar characteristics post burn injury.

Key words: Wound healing, Burn injury, Scarring, Skin 11β-HSD1, 11β-HSD1 knockout, Glucocorticoid metabolism, Polycaprolactone scaffold, Drug delivery

Highlights

- Knocking out 11β-HSD1 activity in skin was found to accelerate wound healing while the healed wounds demonstrated more collagen deposition and myofibroblast formation, which caused excessive scarring.
- Application of inactive glucocorticoid reactivated by 11β-HSD1 activity in burn injury significantly reduced post-burn scarring via reductions in inflammation, myofibroblast generation, collagen production and scar stiffness.
- Controlled delivery of an inactive glucocorticoid that could only be reactivated within skin cells expressing 11β-HSD1 is a novel therapeutic approach to improve wound healing and scar qualities.
- Utilizing the 11β-HSD1 system, direct adverse effects associated with overuse of topically applied active glucocorticoids are expected to be minimized. This information provides the logical basis for clinical trials of treatments designed to reduce the adverse features of burn injury wound healing.

Background

Burn injuries are complex and under-appreciated traumatic injuries that lead to various local and systemic effects associated with immune and inflammatory response and metabolic reactions [1, 2]. Additionally, post-burn scarring is the most common and severe functional consequence affecting burn injury survivors [3, 4]. Individuals with severe scarring experience significant problems in eating, breathing and mobility. Moreover, the aesthetic issues associated with post-burn scarring cause a considerable long-term psychological impact [5]. Abnormal scar formation is caused by an excessive inflammatory response, exaggerated fibroblast activity and the disorganized over-production of collagen [6, 7]. Current treatments for scarring include surgical approaches, pressure garments, radiotherapy, cryotherapy and laser therapy. However, in controlled studies these treatments have minimal or no effects on post-burn scarring [8, 9].

Glucocorticoids are used to treat a variety of skin diseases, including alopecia areata, pruritus, atopic dermatitis and burn injury, on the basis of their anti-inflammatory and immune-modulating activities [10, 11]. Intralesional glucocorticoid injections have also been used to prevent and manage scarring since the mid-1960s [8, 12]. However, long-term use of glucocorticoids results in adverse effects, such as adrenal suppression, glucose intolerance, increased protein catabolism and breakdown, increased susceptibility to infection and classic features of Cushing's syndrome [12].

Glucocorticoid excess in skin leads to skin thinning/atrophy, decreased collagen deposition, violaceous striae, easy bruising and poor wound-healing post injury [13, 14]. Local activation of glucocorticoids in skin tissue can occur via the 11β-hydroxysteroid dehydrogenase type 1 enzyme (11β-HSD1) [15].11β-HSD1 is an NADP(H)-dependent enzyme that catalyses the bidirectional conversion of cortisol (active) and cortisone (inactive) but predominantly activates glucocorticoids from their inactive forms [16]. 11β-HSD1 is expressed in a variety of tissues, such as liver, adipose tissue, nervous system, bone and skin as well as inflamed tissue [17]. In skin, 11β-HSD1 expression has been reported in keratinocytes and dermal fibroblasts [18, 19]. 11β-HSD1 primarily activates cortisone to cortisol, while increased 11β-HSD1 activity is associated with greater production of active glucocorticoids in skin [20]. 11β-HSD2 by contrast inactivates cortisol to cortisone. Although 11β-HSD2 is also expressed in skin it is largely found in sweat glands [21]. Mice with genetic knockout (KO) of 11β-HSD1 in skin have been demonstrated to have accelerated cutaneous (non-burn) wound healing, with healed wounds having greater production of collagen [22–25]. Although more collagen generation is generally considered beneficial for simple wound healing, e.g. in chornic wound healing with diabetics [26], excessive collagen production would be detrimental to scar formation after burn injury [27].

Previous studies found that the tissue level of cortisol, the predominant glucocorticoid in humans, was elevated in subcutaneous tissue in burn injury patients compared to healthy volunteers [28]. However, the role of glucocorticoid metabolism via 11β-HSD1 in burn injury has not previously been examined. In the present study, we therefore examined changes in local expression and activity of 11β-HSD1 in skin after burn injury in both humans and mice. We aimed to investigate the local impact of 11β-HSD1 on burn wound healing,

scar formation and scar mechanical features using a mouse model with 11β-HSD1 global KO. Furthermore, we also developed and pre-clinically tested the effect of slow-release scaffolds encapsulating active or inactive glucocorticoids on the healing of burn injury in mice. We hypothesised that 11β-HSD1 would be an important suppressor of collagen production and scar tissue formation, and that modulation of local glucocorticoid activation via 11β-HSD1 within skin could be utilized to improve the qualities of scars formed post burn injury.

Methods

Human tissue

All human skin samples were collected from the Burns & Reconstructive Surgery Unit, Concord Hospital, Australia. The protocol was approved by Sydney Local Health District (Concord) Human Research Ethics Committee (CH62/6/2014-139). Burn injury affected skin tissues were collected from burn injury patients [aged 16–72 years; 0.5–90% total body surface area (TBSA); 1–42 days post burn injury]. The patients information, including their gender, age, %TBSA and time of postburn are shown in Table S1 (see online supplementary material). Each skin sample was divided into two. One part was kept in 10% neutral buffered formalin solution (Sigma-Aldrich) for histological analysis and the part was temporarily kept in RNAlater Stabilization Solution (Life Technologies) immediately after the procedure and then stored at −80°C for mRNA expression analysis.

Global 11β-HSD1 KO mouse model

Global 11β-HSD1 KO mice were generated on a C57/BL6 background by breeding 11β-HSD1 floxed mice with Sox2-Cre mice as previously described [29, 30]. In the present study, global 11β-HSD1 floxed mice were generated at the Institute of Metabolism and Systems Research, University of Birmingham, UK and introduced to the Translational Research Facility at the ANZAC Research Institute, Australia. Sox2-Cre transgenic mice were purchased from Australian BioResources, Australia. In this model, Cre recombinase is expressed under the control of the mouse Sox2 promoter in Sox2-Cre mice. The activated Sox2 promoter produces Cre recombinase to cleave loxP-flanked exon 5 of the 11β-HSD1 gene (HSD11B1) (Figure S1, see online supplementary material). The transgenic mice used in this study were all toe-clipped and genotyped at the age of 2–3 weeks using the primers listed in Table 1. The breeding protocols and strategies have been approved by Sydney Local Health District Animal Welfare Committee (Protocol No 2013/074 and 2019/035).

Burn injury mouse model

The burn injury mouse model was established as previously described [31]. Male wild type (WT) mice (aged 10–12 weeks, n = 6–8/group/timepoint) and male mice with global KO of 11β-HSD1 (generated in house; aged 10–12 weeks, n = 6/group/timepoint) were used for the burn injury study. Each animal was subjected to a hot brass rod at around 230°C for 10 s to create a full-thickness small burn injury with 1 cm^2 wound size (∼5% TBSA). Each burned mouse was housed in a single standard cage with free access to food and water in the Translational Research Facility of the ANZAC Research Institute, where the environment was controlled at 24–26°C and 44–46% humidity under a 12:12 h light–dark cycle. Mice were given 1 ml of warm resuscitative intraperitoneal saline and analgesia (buprenorphine 0.05 mg/kg) via intraperitoneal injection for 2 days after burn injury. All protocols were approved by the Sydney Local Health District Welfare Committee (Protocol No. 2018/020) under Australian National Health and Medical Research Council Guidelines for animal experimentation. The damaged skin on mice underwent debridement 2 days after burn and was covered with a wound dressing for 7 days, aiming to reduce the risk of wound infection. Wound size was measured at different timepoints until the wound was completely closed. Groups of mice were anaesthetized with ketamine/xylazine (100 mg/100 mg/kg) and euthanised by cervical dislocation at different timepoints and their skin and wound tissues were harvested and bisected for histology and gene expression analysis, respectively.

Histology

Tissues were embedded in paraffin and sectioned at a thickness of 5 μm. Paired sections at different timepoints were cut per slide and stained with hematoxylin and eosin (H&E) for analysis of wound structure and area. Multiple sections of day 49 scar tissues were stained with Masson's Trichrome to measure the percentage of positively stained collagen fibres using Fiji—ImageJ [32].

Immunohistochemistry

11β-HSD1, proliferating cell nuclear antigen (PCNA) and α-smooth muscle actin (α-SMA) protein expression in skin and wound sections were analysed using primary antibodies (Abcam), an ABC Kit (Vector Laboratories) and DAB Substrate (Vector Laboratories). Antigen retrieval was undertaken using a commercial antigen retrieval buffer, Diva decloaker (Biocare Medical) and a heat-induced epitome retrieval machine, Decloaking chamber (Biocare Medical) with a temperature setting of 110°C for 15 min. The tissues were then incubated with each primary antibody overnight in the fridge. The next day, tissue sections were incubated with a secondary goat anti-rabbit IgG antibody followed by the ABC kit and DAB kit techniques (Vector Laboratories), based on the manufacture's instruction. The slides were then counterstained and mounted. The assessment of immunohistochemistry (IHC) staining was conducted by three independent researchers who were blind to the identity of samples. PCNA-positive cells were counted when

Table 1. Primer sequences for Cre and 11β-HSD1 KO genotyping

Primer	Sequence (forward, 5′ to 3′)	Sequence (reverse, 5′ to 3′)
Cre	GCGGTCTGGCAGTAAAAACTATC	GTGAAACAGCATTGCTGTCACTT
IPC	CTAGGCCACAGAATTGAAAGATCT	GTAGGTGGAAATTCTAGCATCATCC
HSD1 Primer 1	CTGGGAGCTTGCTTACAGCATCA	
HSD1 Primer 2	CATTCTCAAGGTAGATTGAACTCTG	
HSD1 Primer 3	AGTCCATGCAATCAACTTCTCGTC	

IPC internal positive control, *HSD1* hydroxysteroid dehydrogenase type 1 enzyme

Table 2. Primer sequences for real-time PCR gene expression analysis

Primer	Sequence (forward, 5′ to 3′)	Sequence (reverse, 5′ to 3′)
Human B2M	AGCAGCATCATGGAGGTTTG	CAAACATGGAGACAGCACTCA
Human 11β-HSD1	TGGCTTATCCAATGGTTGC	CTATCCCAGAAACTGCCTTCA
Mouse RPL19	GATCATCCGCAAGCCTGTGACT	GTGCTTCCTTGGTCTTAGAC
Mouse 11β-HSD1	GGAGCCGCACTTATCTGAA	GACCTGGCAGTCAATACCA
Mouse TNF-α	TAGCCCACGTCGTAGCAAAC	GCAGCCTTGTCCCTTGAAGA
Mouse IL-1β	TGCCACCTTTTGACAGTGATG	TGATGTGCTGCTGCGAGATT
Mouse TGF-β1	CTTTAGGAAGGACCTGGGTT	CAGGAGCGCACAATCATGTT
Mouse PCNA	TGTGCCCCTTGTTGTAGAGT	AAAGACCTCAGGACACGCTG
Mouse α-SMA	AGCCATCTTTCATTGGGATGG	CCCCTGACAGGACGTTGTTA
Mouse COL1α1	CCAGTGGCGGTTATGACTT	GCGGATGTTCTCAATCTGC
Mouse COL3α1	CCCAACCCAGAGATCCCATT	GAAGCACAGGAGCAGGTGTAGA

B2M beta-2 microglobulin, *RPL19* ribosomal protein L19, *11β-HSD1* 11β-hydroxysteroid dehydrogenase type 1 enzyme, *IL-1β* interleukin 1 beta, *TNF-α* tumour necrosis factor-α, *TGF-β1* transforming growth factor beta 1, *PCNA* proliferating cell nuclear antigen, *α-SMA* α-smooth muscle actin, *COL1α1* type I collagen, *COL3α1* type III collagen

the nuclei of cells lying on the basement membrane in the extending epidermal tongue were stained dark brown. α-SMA expression was quantified by Fiji—ImageJ and is presented as the percentage of positively DAB-stained area [33].

RNA extraction and real-time-PCR gene expression analysis

The wound tissues collected from different timepoints post burn were stored at −80°C prior to RNA extraction. mRNA from skin and wound tissues was extracted using TRI-Reagent (Sigma Aldrich) according to the manufacturer's instructions. Total mRNA (1 μg) was reverse transcribed to complementary DNA using a SensiFAST cDNA synthesis kit (Bioline). Real-time PCR analysis was conducted using SsoAdvanced Universal SYBR Green Supermix (Bio-Rad). Primer sequences designed by Primer-BLAST Software are shown in Table 2. The efficiency of DNA amplification was evaluated using the mean cycle threshold (Ct) method. ΔCt value was calculated from Ct values of different interest genes by subtracting the Ct value of the housekeeping gene beta-2 microglobulin for human samples and ribosomal protein L19 for mouse samples. The resulting relative mRNA expression is shown as fold-change ($2^{-\Delta\Delta Ct}$) relative to the expression in baseline samples.

Mechanical property testing

Mechanical property testing using a Bioplus mechanical tester was optimized and performed in the School of Chemical and Biomolecular Engineering, University of Sydney. Fresh scar tissues collected from WT and 11β-HSD1 KO mice on day 49 after burn injury were cut into 20 × 50 mm strips and mounted between the grips of the machine. Testing was performed at a speed of 10 mm/min. Stress–strain curves were created by calculating the force applied on a sample (tensile strength) and the displacement of a sample. The data are expressed as Young's modulus and tensile strength.

Fabrication of drug-loaded polycaprolactone/collagen scaffolds by electrospinning

Polycaprolactone (PCL)/collagen electrospun scaffolds are well validated in the Burns Research Group as previously described [34–36]. For preparing scaffolds, 25 mg of dry rat type I collagen (COL1α1; 2.5% w/v) and 75 mg of PCL (7.5% w/v) were dissolved in 1 ml of hexafluoro-2-propanol (HFP) as the placebo scaffold. The therapeutic agents including prednisolone and prednisone were encapsulated in PCL/-collagen scaffolds. The concentration of prednisolone and prednisone was determined on the basis of previous literature [37–39]. Prednisolone (5 mg; 0.5% w/v) and prednisone (5 mg; 0.5% w/v) were added in 1 ml of HFP with 7.5% PCL and 2.5% collagen, respectively. The electrospinning parameters were optimized with the following conditions: flow rate of 1 ml/h; 20 cm air gap; applied electric potential (8 kV and 10 kV). During electrospinning, 0.5 ml of mixed solution was loaded into a 1 ml syringe with a blunt, 18-gauge needle attached. A positive charge was connected to the needle and a negative charge to the bronze collector. When an electric potential is applied, charge accumulates to form

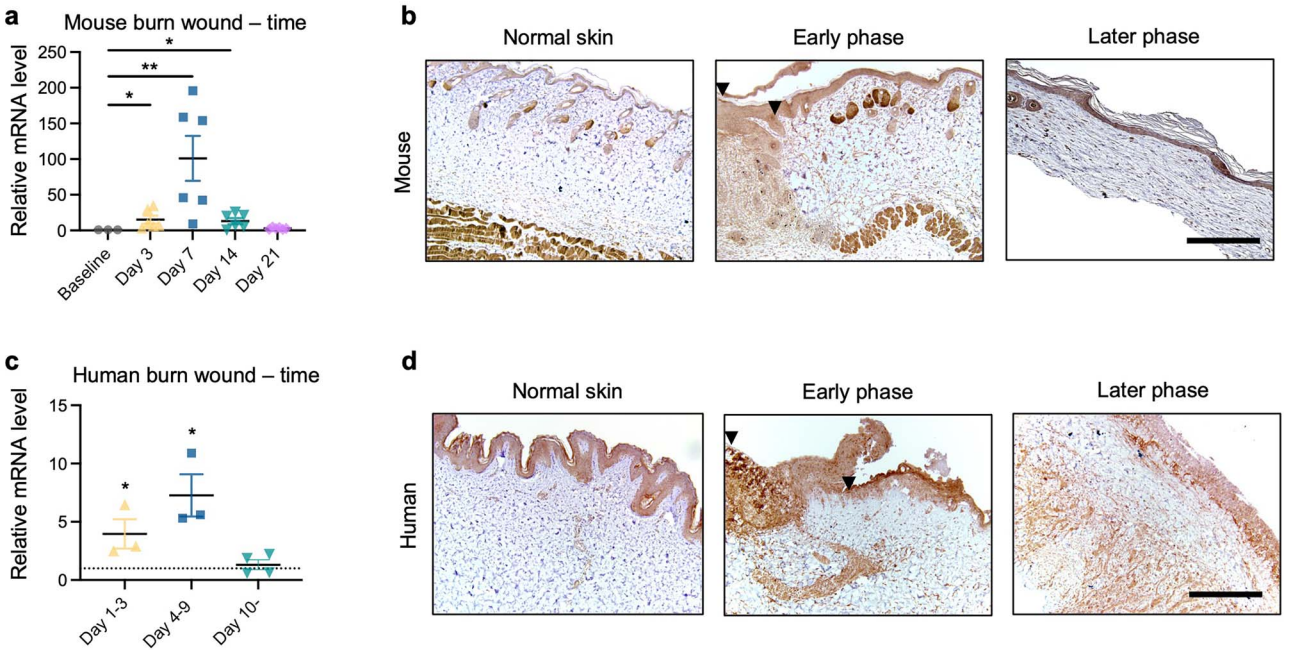

Figure 1. 11β-HSD1 mRNA and protein expression in skin and wound tissues after burn injury. (**a**) RT-PCR analysis of 11β-HSD1 in mouse burn wound tissues grouped by days post burn injury. $n=3$ in the baseline groups. $n=6$ per group per timepoint. Bars represent means ± SEM; $^{*}p<0.05$, $^{**}p<0.01$ relative to baselines. Data was analysed by one-way analysis of variance (ANOVA). (**b**) Immunohistochemical images of 11β-HSD1 in mouse normal skin tissues and burn wound tissues. Arrowheads indicate the wound site (Scale bar: 500 μm). (**c**) RT-PCR analysis of 11β-HSD1 in human burn wound tissues grouped by days post burn injury. $n=3$ in group days 1–3 and 4–9 and $n=4$ in group day 10–. Bars represent means ± SEM; $^{*}p<0.05$ relative to baselines. Data was analysed by one-way ANOVA. (**d**) Immunohistochemical images of 11β-HSD1 in human normal skin tissues and burn wound tissues. Arrowheads indicate the wound site (Scale bar: 500 μm). *11β-HSD1* 11β-hydroxysteroid dehydrogenase type 1 enzyme

the electric field between the needle and the collector. When the force of the electric field exceeded the cohesive force of the solution, an electrically charged jet of scaffold solution erupted and moved towards the collector plate. The HFP solvent evaporated and the elongated jet solidified into fibres and formed a non-woven porous structure on the collector [40]. After 5 min of air drying, the scaffolds were removed from the collector using fine-tipped forceps.

Statistics

Experimental data were analysed by GraphPad Prism software (Graph-Pad). One-way analysis of variance (ANOVA) and the Holm–Šídák post hoc test was used for single-factor analysis. Studies comparing more than three groups of two factors were analysed using two-way ANOVA. Data are expressed as mean ± SEM. The null hypothesis was rejected at a significance level of $p<0.05$ ($^{*}p<0.05$; $^{**}p<0.01$; and $^{***}p<0.001$).

Results

11β-HSD1 expression in burn-affected and donor-site (non-burn) skin collected from burn injury mice and patients

11β-HSD1 mRNA expression was first analysed in the burn wounds collected from burn injury mice. When mouse burn wound samples were grouped by days postburn (Figure 1a), the relative mRNA levels of 11β-HSD1 were substantially increased after burn injury on days 3, 7 and 14 (15.2 ± 5.5, 101.0 ± 31.6 and 13.1 ± 4.2-fold significant increase, respectively: $p<0.05$ baseline *vs* days 3 and day 14 ; $p<0.01$ baseline *vs* day 7). IHC analysis of 11β-HSD1 demonstrated that higher protein expression of 11β-HSD1 was present in mouse wound area after burn injury compared to normal skin (Figure 1b). Keratinocytes in the epidermis were the most common cell type that expressed 11β-HSD1 in normal skin. After burn injury, a variety of cell types including keratinocytes, leukocytes and fibroblasts (Figure S2, see online supplementary material) highly expressed 11β-HSD1 at the wound site. These observations were similar in human tissue post burn injury. Compared to the tissue from healed burn wounds (designated basal/baseline), human wounds immediately after burn injury demonstrated significantly higher 11β-HSD1 mRNA levels (4.0 ± 1.3-fold increase on days 1–3 and 7.3 ± 3.1-fold increase on days 4–9 compared to baselines; $p<0.01$) (Figure 1c). After 10 days postburn, the expression declined to the baseline level. IHC analysis of 11β-HSD1 in human burn wounds demonstrated changes consistent with IHC analysis in mouse burn wounds (Figure 1d). A considerable increase in 11β-HSD1 expression was observed in mouse wound areas at the early phase of wound healing, especially in the dermal layer. These findings suggest that both mRNA level and protein expression of 11β-HSD1 in skin could be stimulated and induced by burn injury in mice and humans.

Impact of 11β-HSD1 KO on burn injury wound healing

We investigated the role of 11β-HSD1 in burn wound healing using global 11β-HSD1 KO mice compared to WT (Figure 2a). Both groups of mice were sacrificed at defined time points after burn injury and tissues were harvested for further analysis. An 11β-HSD1 activity assay and serum corticosterone assays were performed to confirm that 11β-HSD1 activity was completely abolished in skin in the 11β-HSD1 KO mice (Figure S3a, see online supplementary material) and that both WT and 11β-HSD1 KO mice had comparable serum corticosterone levels after burn injury (Figure S3b, see online supplementary material), suggesting that global KO of 11β-HSD1 had no effect on systemic levels of glucocorticoids following burn injury. As such, 11β-HSD1 KO will only be expected to have local impacts on wound healing with no impact on systemic glucocorticoid levels.

After the mice were subjected to burn injury, a significant reduction in wound area was observed in 11β-HSD1 KO mice on days 7 and 14 based on macroscopic photographic analysis when compared to WT mice (Figure 2b). Using a quantitative analysis of wound area (Figure 2c), mice of 11β-HSD1 KO background demonstrated significantly accelerated wound healing on days 3 and 7 after burn compared to WT mice (-9.2 ± 2.7% baseline area healed in WT *vs* 4.0 ± 5.2% KO on day 3, and 28.3 ± 4.2% WT *vs* 45.3 ± 2.6% KO on day 7). Both WT and 11β-HSD1 KO mice achieved ~80% wound closure on day 14 and both completed wound closure on day 21. H&E staining showed a larger wound area in WT mice compared to 11β-HSD1 KO mice on day 14 (Figure 2d).

The post-burn inflammatory response in wounds of WT and 11β-HSD1 KO mice was assessed by examining mRNA expression of pro-inflammatory cytokines, tumour necrosis factor alpha (TNF-α), interleukin 1 beta (IL-1β) and transforming growth factor beta 1 (TGF-β1) on days 3 and 7 (Figure 2e). Significantly higher mRNA levels of IL-1β and TNF-α were found in 11β-HSD1 KO mice compared to WT mice on day 3 post burn (12.1 ± 2.6-fold WT *vs* 33.1 ± 7.0-fold KO mice for IL-1β, and 3.6 ± 0.8-fold WT *vs* 10.5 ± 1.7-fold KO for TNF-α). TGF-β1 mRNA levels were increased by ~2-fold in both WT mice and 11β-HSD1 KO mice on day 3 and 1.5-fold on day 7. However, no significant difference in TGF- β1 levels was found between WT mice and 11β-HSD1 KO mice at each timepoint. In the proliferation phase of wound healing, wound tissues in WT mice and 11β-HSD1 KO mice showed increased PCNA mRNA expression relative to baselines on days 3 and 7 post burn injury (1.5 ± 0.1-fold increase WT and 1.8 ± 0.1-fold increase KO on day 3; 1.6 ± 0.1-fold increase WT and 2.1 ± 0.2-fold increase KO on day 7) (Figure 2f). Significant differences between WT and KO were found on days 3 and 7. mRNA levels of ACTA (α-SMA) were also found to be enhanced after burn injury. Compared to WT mice, 11β-HSD1 KO mice showed significantly higher levels of ACTA mRNA in wounds on day 7 postburn (1.7 ± 0.2-fold increase WT *vs* 4.2 ± 0.7-fold increase KO; $p < 0.01$).

IHC staining of PCNA and α-SMA was performed to confirm cell proliferation of keratinocytes (Figure 2g) and myofibroblast differentiation in wound tissues on days 7 and 14 post burn injury. WT mice and 11β-HSD1 KO mice had 32 ± 5 and 37 ± 4% of positive stained keratinocytes, respectively, on days 7 and 32 ± 5 and 38 ± 6% on day 14 (Figure 2h). Although protein expression analysis did not show significant differences between WT and KO, the trend was consistent in mRNA expression and protein expression by IHC that KO mice had higher expression of PCNA in wounds compared to WT mice. α-SMA IHC images demonstrated that 11β-HSD1 KO wounds had a greater intensity of positive α-SMA expression than WT wounds on days 3 and day 7 (Figure 2i). By quantifying the α-SMA protein expression (Figure 2j), 11β-HSD1 KO mice had ~20% on day 3 and 19% on day 7 greater α-SMA protein expression at the wound site compared to WT mice. These findings indicate that 11β-HSD1 KO promotes increased myofibroblast differentiation after burn injury.

11β-HSD1 knockout exacerbates post-burn scarring and fibrosis with excessive collagen production and increased stiffness

Compared to WT mice, 11β-HSD1 KO mice were shown to have significantly higher type III collagen (COL3α1) mRNA levels on day 3 (0.7 ± 0.1-fold WT *vs* 1.5 ± 0.1-fold KO) and COL1α1 on days 14 and 28 in wounds (3.2 ± 1.0-fold WT *vs* 19.6 ± 2.7-fold KO on day 14 and 5.8 ± 1.0-fold WT *vs* 14.4 ± 2.0-fold KO on day 28) (Figure 3a). Histological analysis of Masson's Trichrome staining further demonstrated significantly denser collagen fibres in a healed wound area of 11β-HSD1 KO mice compared to WT mice on day 49 (Figure 3b). Scar tissues collected from 11β-HSD1 KO mice were found to have an average 15% more connective tissues than WT mouse scars (Figure 3c). The mechanical properties of mature scars on day 49 in WT and 11β-HSD1 KO mice were measured using an Instron Bioplus Mechanical Tester (Figure 3d). Stress–strain curves were plotted based on the stress needed to break a sample (tensile strength) and the strain on a sample when it breaks (% elongation to breaking point). Scar tissues in 11β-HSD1 KO mice had 2-fold higher Young's modulus compared to WT mice (Figure 3e), indicating scar tissues in 11β-HSD1 KO mice were significantly stiffer than those in WT mice. A higher tensile strength was also detected in fresh scar tissues from 11β-HSD1 KO mice, indicating a greater ability to absorb more energy before breaking.

Impact of prednisolone and prednisone on wound healing

The surface morphology of prednisolone and prednisone electrospun scaffolds was analysed via scanning electron microscopy (Figure S4a,b, see online supplementary material). No drug particles were detected on the external surface of each scaffold. There was no difference noted in pore

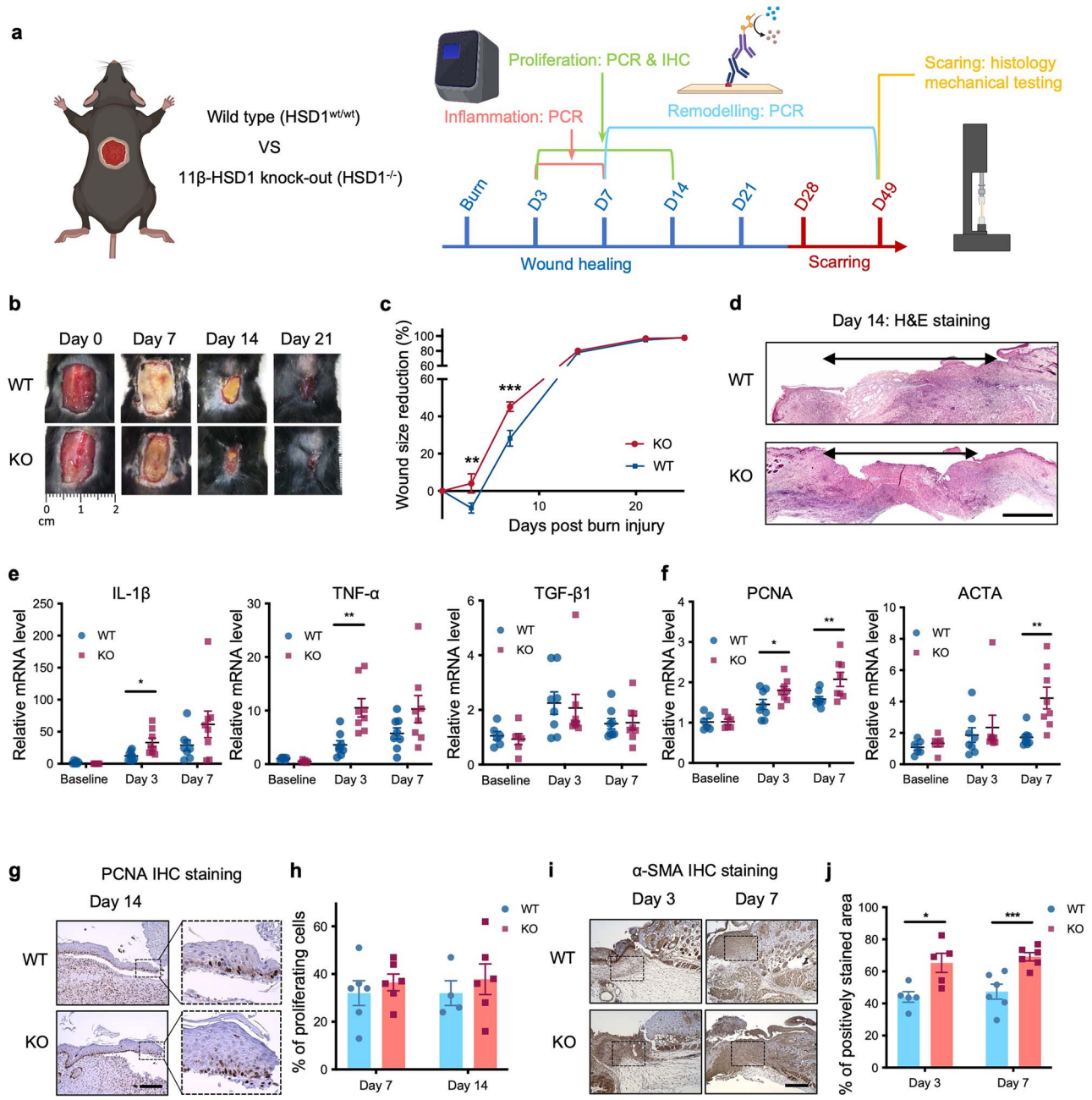

Figure 2. Impact of 11β-HSD1 KO on the wound healing process. (**a**) C57BL/6 WT mice and 11β-HSD1 KO mice were subjected to burn injury and examined for wound healing and scarring post burn injury. Created with BioRender.com. (**b**) Digital photos of wounds in the WT and 11β-HSD1 KO mice. (**c**) Wound size reduction rate was quantified by Image J over 25 days after burn injury. $n = 6$ per group per time point. (**d**) Illustration of the whole wound area in WT and 11β-HSD1 KO mice on day 14 by stitching multiple H&E staining images. Double-headed arrow indicates the open wound (Scale bar: 1000 μm). (**e**) RT-PCR analysis of pro-inflammatory cytokines IL-1β, TNF-α and TGF-β1 in wound tissues of WT and 11β-HSD1 KO mice. $n = 6$ in the baseline group. $n = 8$ in the WT and 11β-HSD1 KO groups per time point. (**f**) RT-PCR analysis of PCNA and ACTA (α-SMA) in WT and 11β-HSD1 KO mouse wounds on days 3 and 7. $n = 8$ in WT and 11β-HSD1 KO groups. (**g**) IHC images of PCNA in the extending epidermal tongues of WT and 11β-HSD1 KO wounds on day 14 (Sale bar: 200 μm). (**h**) Assessment of keratinocyte proliferation by counting the number of PCNA-active cells per 30 cells. $n = 4$–6 in WT and 11β-HSD1 KO groups on days 7 and 14. (**i**) IHC images of α-SMA in WT and 11β-HSD1 KO mouse wounds on days 3 and 7 (Scale bar: 500 μm). (**j**) Quantification of α-SMA-positive area in wounds. $n = 5$–6 in WT and 11β-HSD1 KO groups. Data are presented as means ± SEM and analysed by ANOVA with multiple comparisons; $^{*}p < 0.05$. $^{**}p < 0.01$ $^{***}p < 0.001$ WT *vs* KO. *11β-HSD1* 11β-hydroxysteroid dehydrogenase type 1 enzyme, *IL-1β* interleukin 1 beta, *TNF-α* tumour necrosis factor-α, *TGF-β1* transforming growth factor beta 1, *PCNA* proliferating cell nuclear antigen, *α-SMA* α-smooth muscle actin, *WT* wild type, *KO* knockout, *IHC* immunohistochemistry, *H&E* hematoxylin and eosin

diameter or fibre width of scaffolds between each group, indicating that each drug can be effectively embedded inside the polymer structure. *In vitro* drug delivery analysis showed that after an initial phase of higher release, there was reliably sustained delivery of prednisolone and prednisone in PBS at ~15 μmol/day (Figure S4c, see online supplementary

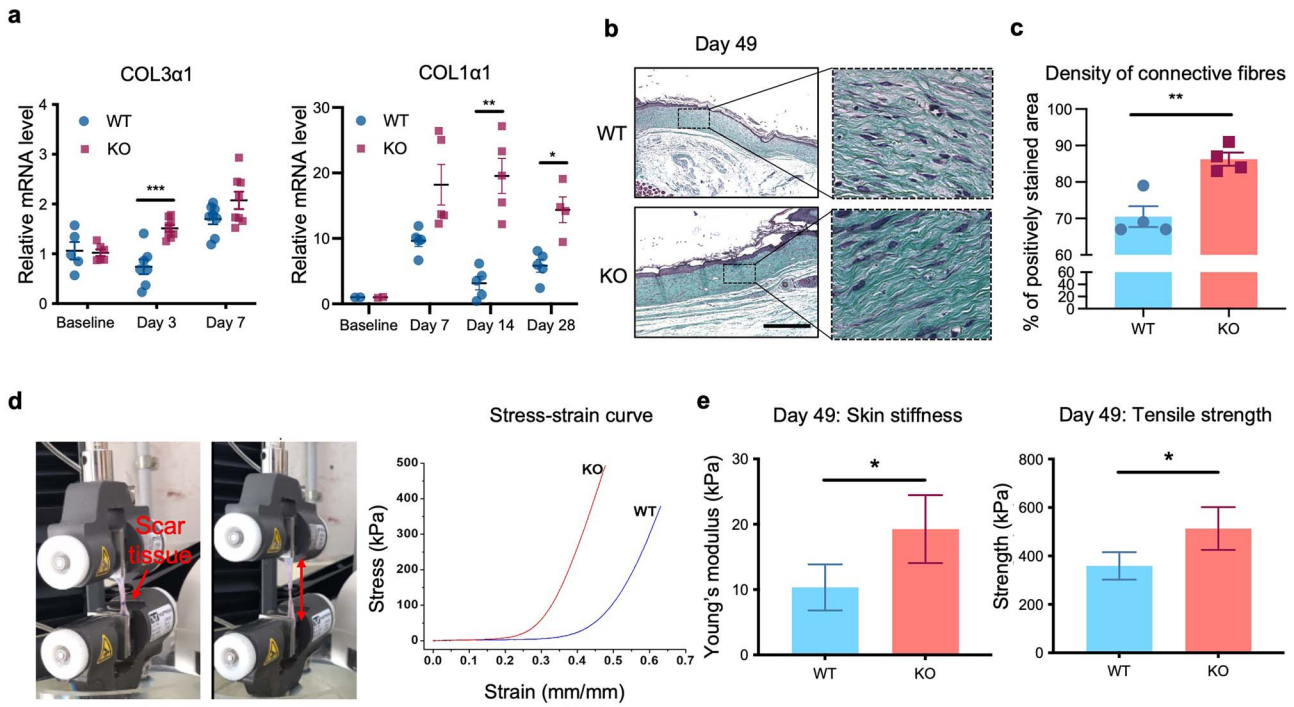

Figure 3. Impact of 11β-HSD1 KO on tissue remodelling and scarring. (**a**) RT-PCR analysis of COL3α1 in wound tissues on days 3 and 7, and COL1α1 on days 7, 14 and 28 post injury. $n=5$–8 per group per timepoint. (**b**) Images of Masson's Trichrome staining in WT and 11β-HSD1 KO mouse scars on day 49. Scale bar, 500 μm. (**c**) Quantification of Masson's Trichrome staining demonstrates the density of connective fibres in WT and 11β-HSD1 KO mouse scars. $n=4$ in the WT and 11β-HSD1 KO groups. (**d**) The mechanical strength and tensile properties of scars from WT and 11β-HSD1 KO mice were examined. The stress-strain curve was created while the scar tissues were being stretched by the applied force until they broke apart (ultimate failure). The gradient of the 11β-HSD1 KO stress/strain curve looked greater/steeper than that of WT curve indicating 11β-HSD1 KO scars were likely to have greater stiffness and elasticity. (**e**) The mechanical testing demonstrates skin stiffness and tensile strength in post-burn scars on day 49. $n=4$ in WT and 11β-HSD1 KO groups. Bars present means ± SEM, analysed by one-way ANOVA; $^*p<0.05$, $^{**}p<0.01$, $^{***}p<0.001$ WT *vs* KO. *11β-HSD1* 11β-hydroxysteroid dehydrogenase type 1 enzyme, *WT* wild type, *KO* knockout, *COL1α1* type I collagen, *COL3α1* type III collagen

material). This level of release would be predicted to be effective over 21 days. Thereafter, WT mice were subjected to burn injury and different scaffolds were applied to the wounds, including placebo scaffolds, prednisolone scaffolds (active glucocorticoid) or prednisone scaffolds (inactive glucocorticoid) (Figure 4a).

Mice in which prednisone and prednisolone scaffolds were applied post burn had larger wound size on days 14, 21 and 28 compared to the mice receiving placebo scaffolds (Figure 4b). Both prednisolone and prednisone significantly delayed wound repair (Figure 4c). Mice treated with placebos reached 50% wound size reduction at day 11 post burn injury, whereas mice treated with either prednisolone-loaded scaffolds or prednisone-loaded scaffolds needed 18 days to heal 50% of wound area. The impact of prednisone on mouse wound healing was found to be slightly greater (but not significantly) compared to prednisolone, the active glucocorticoid, suggesting that the inactive glucocorticoid had been successfully reactivated by burn injury-induced activity of 11β-HSD1 in skin.

The mRNA levels of pro-inflammatory cytokines, IL-1β, TNF-α and TGF-β1 in wound tissues were examined on day 3 (Figure 4d). Compared to prednisolone, prednisone treatment suppressed TNF-α and IL-1β expression more significantly in wound tissues (0.9 ± 0.3-fold prednisolone *vs* 0.5 ± 0.1-fold prednisone for TNF-α, and 0.8 ± 0.3-fold prednisolone *vs* 0.3 ± 0.1-fold prednisone for IL-1β). mRNA levels of TGF-β1 in wounds were also found to be significantly decreased by treatment with both prednisolone and prednisone (0.6 ± 0.3-fold decrease prednisolone and 0.6 ± 0.1-fold decrease prednisone relative to placebo). These findings demonstrate that the early inflammatory response in burn injury was more effectively suppressed via local application of prednisone, effects not seen in the group receiving prednisolone scaffolds.

In the cell proliferation phase of wound healing, prednisolone scaffolds had minor effects on PCNA and ACTA (α-SMA) mRNA expression (Figure 4e), while wounds treated with prednisone manifested significantly lower PCNA mRNA levels compared to placebo wounds on day 3 (0.7 ± 0.03-fold decrease in prednisone compared to placebo) as well as significantly decreased ACTA mRNA expression on day 7 (0.6 ± 0.05-fold decrease on day 7 post burn compared to placebo).

Protein expression of PCNA was detected in epidermal keratinocytes of mice treated with placebo, prednisolone and prednisone in IHC images (Figure 4f). Mice having different treatments showed no significant difference in cell proliferation of keratinocytes (Figure 4g). IHC analysis of

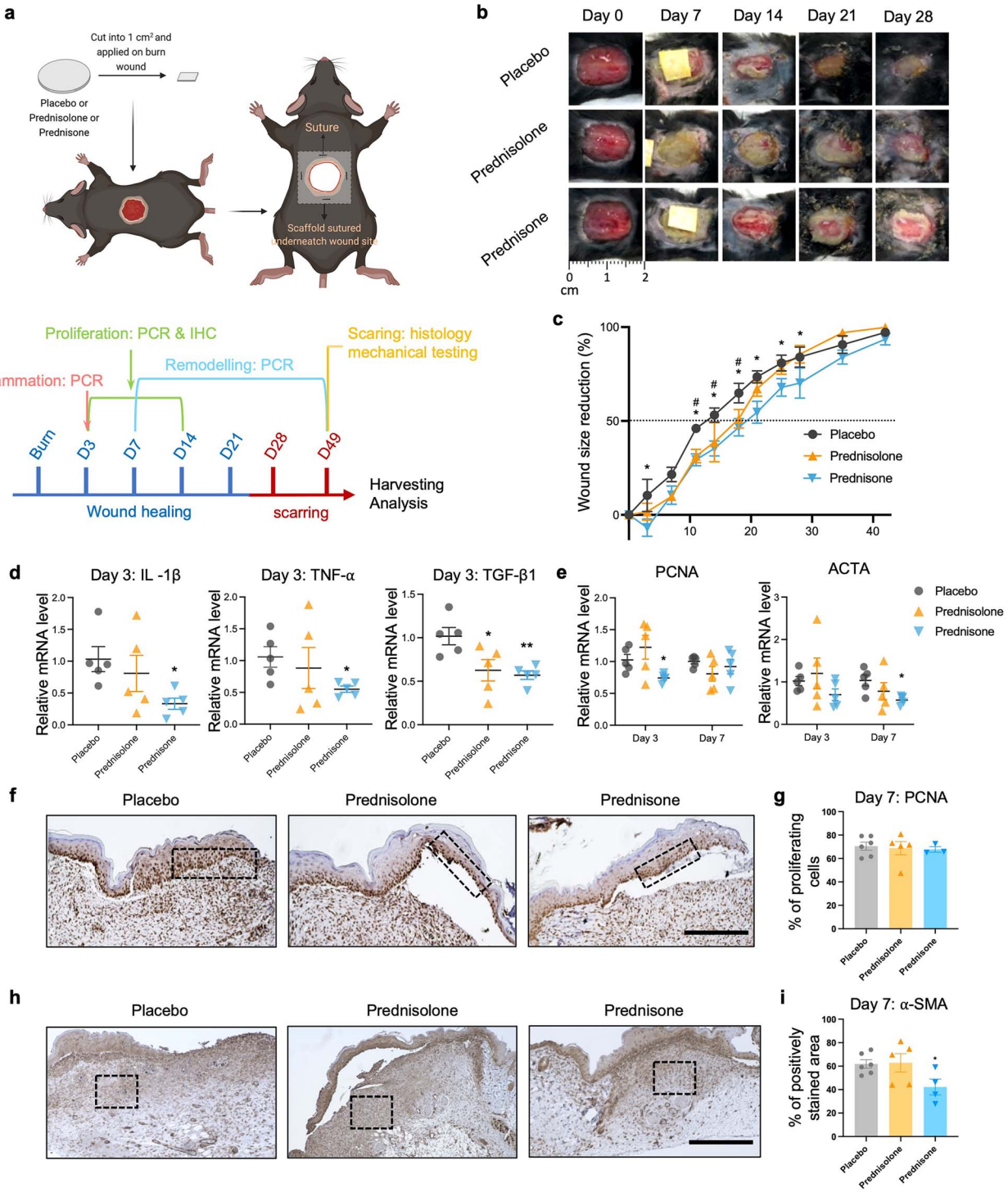

Figure 4. Impact of prednisolone and prednisone on the wound-healing process. (**a**) After burn injury, wounds were debrided and covered with scaffolds containing different therapeutic agents. Created with BioRender.com. (**b**) Digital photos of wounds in the placebo-, prednisolone- and prednisone-treated mouse. (**c**) Wound size reduction rate over 42 days was quantified by Image J. $n = 5$–6 per group per time point. Data are presented as means ± SEM; $^{*}p < 0.05$ placebo *vs* prednisone; #$p < 0.05$ placebo *vs* prednisolone. (**d**) RT-PCR analysis of pro-inflammatory cytokines IL-1β, TNF-α and TGF-β1 in wound tissues treated with placebo, prednisolone and prednisone scaffolds on day 3 post burn. $n = 5$ per group. (**e**) RT-PCR analysis of PCNA and ACTA (α-SMA) in wound tissues on days 3 and 7. $n = 5$ per group per time point. (**f**) IHC images of PCNA in wounds on day 7 (Scale bar: 200 μm). (**g**) Assessment of keratinocyte proliferation by counting the number of PCNA-active cells per 30 cells. $n = 3$–6 in each group. (**h**) IHC images of α-SMA in wounds on day 7 (Scale bar: 500 μm). (**i**) Quantification of α-SMA-positive area in wounds. $n = 5$–6 per group. Bars represent means ± SEM, analysed by ANOVA with multiple comparisons; $^{*}p < 0.05$. $^{**}p < 0.01$ relative to baselines. *11β-HSD1* 11β-hydroxysteroid dehydrogenase type 1 enzyme, *IL-1β* interleukin 1 beta, *TNF-α* tumour necrosis factor-α, *TGF-β1* transforming growth factor beta 1, *PCNA* proliferating cell nuclear antigen, *α-SMA* α-smooth muscle actin, *WT* wild type, *KO* knockout, *IHC* immunohistochemistry

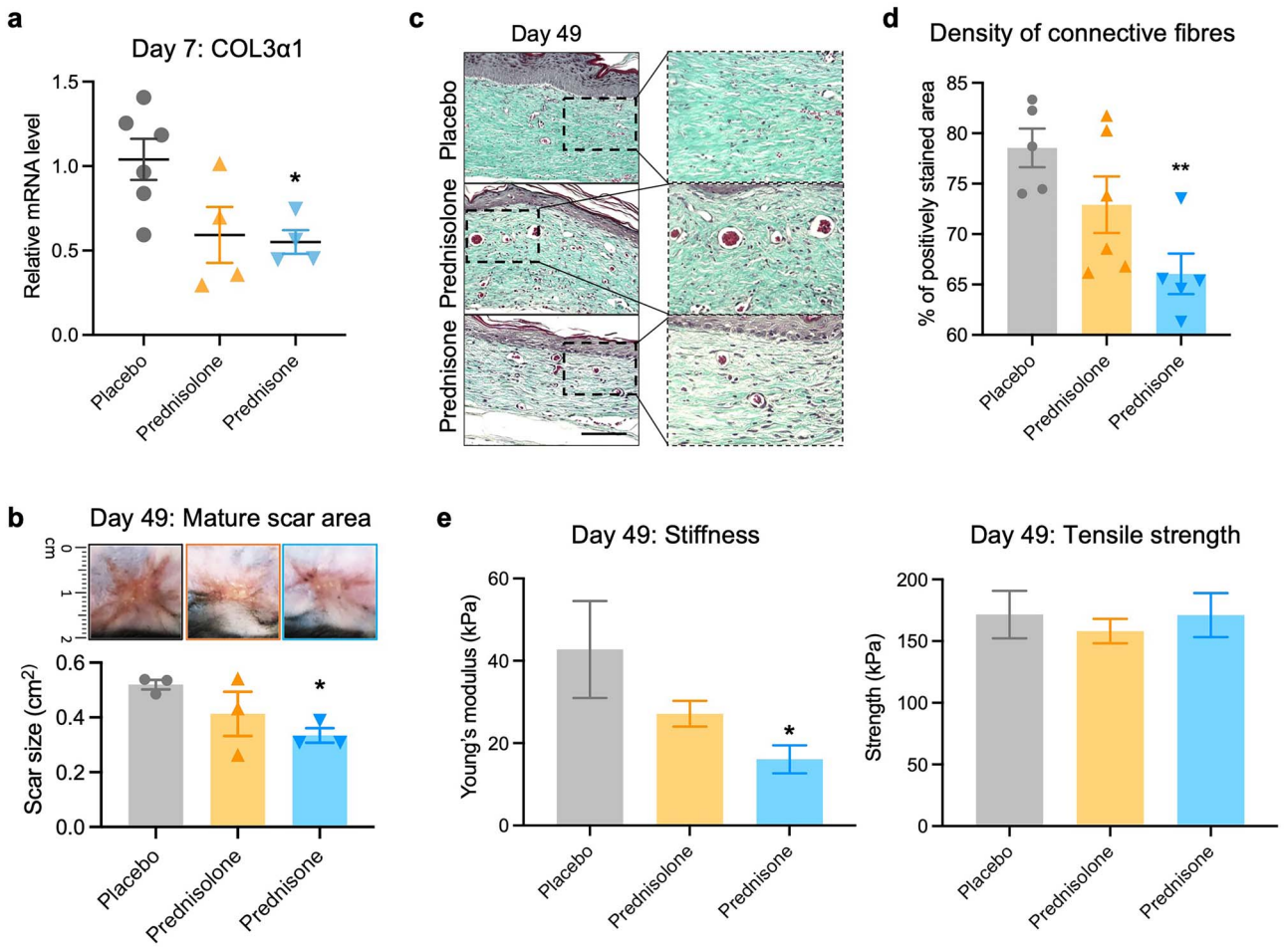

Figure 5. Impact of prednisolone and prednisone on tissue remodelling and scarring. (**a**) RT-PCR analysis of COL3α1 in wound tissues on day 7. $n=4$–5 per group. (**b**) Area of prednisolone- and prednisone-treated scars on day 49. $n=3$ per group. (**c**) Images of Masson's Trichrome staining in scar tissues on day 49. Scale bar: 200 μm. (**d**) Quantification of Masson's Trichrome staining demonstrates the density of connective fibres in mouse scars treated with placebo, prednisolone and prednisone scaffolds. $n=5$ in each group. (**e**) Skin stiffness and tensile strength in mature scars on day 49. $n=4$ in placebo group and $n=7$ in the prednisolone and prednisone group. Bars graphs present means ± SEM, analysed by one-way ANOVA; $^{*}p<0.05$, $^{**}p<0.01$ relative to the placebo group. *COL3α1* type III collagen, *ANOVA* analysis of variance

α-SMA on day 7 showed that mice in the group receiving prednisone treatment had the lowest protein expression of α-SMA detected compared to placebo and prednisolone treatments (Figure 4h) ($42\pm7\%$ of α-SMA-positive area in prednisone-treated wounds compared to $62\pm4\%$ in placebo wounds and $63\pm8\%$ in prednisolone-treated wounds) (Figure 4i). This finding together with the results of α-SMA mRNA expression studies indicates that prednisone treatment suppressed myofibroblast differentiation during the remodelling phase of wound healing.

Prednisone scaffolds significantly reduced collagen production, connective tissue density and stiffness in post-burn scars

Although there was a trend towards prednisolone inhibiting COL3α1 gene expression, only prednisone demonstrated a strong and significant inhibition of COL3α1 when examined on day 7 (Figure 5a). On day 49 post burn, significantly smaller scar areas were observed in mice treated with prednisone (Figure 5b). Compared to placebo mice that had 0.5 ± 0.02 cm^2 scar size, mice treated with prednisone had a significantly smaller size of mature scars with 0.3 ± 0.03 cm^2 in size ($p<0.05$). A trend towards reduction in scar area with prednisolone was not statistically significant. Masson's Trichrome staining revealed that after prednisone-scaffold treatment, scars had a lower collagen fibre density compared to placebo- and prednisolone-treated wounds (Figure 5c), a finding further confirmed by quantitative analysis, with $66\pm2\%$ connective tissue area in prednisone-treated scars *vs* $79\pm2\%$ in placebo scars and $73\pm3\%$ in prednisolone-treated scars (Figure 5d).

Mechanical property testing, in terms of scar stiffness and tensile strength, demonstrated that only scars treated with prednisone produced significantly reduced skin stiffness compared to placebo-treated scars (27 ± 3 kPa prednisolone and 16 ± 3 kPa prednisone *vs* 43 ± 12 kPa placebo) (Figure 5e). Interestingly, scars treated with placebo, prednisolone or prednisone scaffolds demonstrated similar tensile strength (172 ± 19 kPa for placebo, 158 ± 10 kPa prednisolone and 171 ± 18 kPa prednisone). This indicated

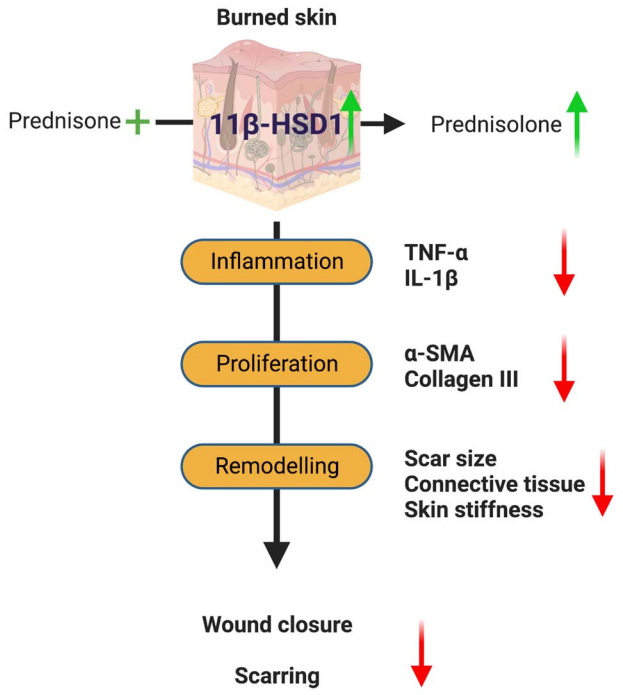

Figure 6. Schematic illustration of the role of 11β-hydroxysteroid dehydrogenase type 1 enzyme (11β-HSD1) in post-burn scarring and the application of prednisone. 11β-HSD1 activity is increased in burn-affected skin. Prednisone in burn injury skin is converted into prednisolone within specific cells expressing 11β-HSD1 and effectively suppresses inflammatory responses, myofibroblast generation and collagen production in the proliferation phase, leading to a slower wound healing rate, decreased scar size, connective tissue accumulation and skin stiffness in final scars Created with BioRender.com. *α-SMA* α-smooth muscle actin, *TNF-α* tumour necrosis factor alpha, *IL-1β* interleukin 1 beta

that prednisone scaffold treatment of burn injury reduced scar stiffness (most likely through reduced collagen density) whilst maintaining scar strength.

These findings elucidate the important role of the 11β-HSD1 in burned skin. The administration of prednisone that could be reactivated by the increased activity of 11β-HSD1 within the skin effectively reduced postburn scarring by downregulating the expression of inflammatory cytokine and scarring-related markers, decreasing connective tissue deposition and reducing adverse mechanical properties (Figure 6).

Discussion

In the present study, we demonstrate that 11β-HSD1 has an important role in wound healing after burn injury. 11β-HSD1 expression restrains post-burn inflammatory responses but also slows down the rate of early phase wound healing assessed by wound area. At a later stage of wound healing 11β-HSD1 expression reduces collagen formation, an effect that was associated with reduced myofibroblast production/differentiation. This information allowed us to use the application of synthetic glucocorticoids to modify the wound healing process and ultimate scar properties in a positive manner. Furthermore, use of an inactive glucocorticoid (prednisone), that was only activated by cells expressing 11β-HSD1, during wound healing resulted in significantly improved final scar qualities.

A role for 11β-HSD1 in cutaneous wound healing has previously been demonstrated but has not before been examined in the context of burn injury [22, 23, 26, 41, 42]. Our results broadly mirror findings from non-burn wound healing studies in the early phase of burn wound healing, with greater rates of wound closure in 11β-HSD1 knockout mice. We however went further to demonstrate an exaggerated local inflammatory response in 11β-HSD1 KO mice with increased levels of TNF-α and IL-1β. Importantly, greater inflammatory responses are implicated in the development of excessive and abnormal scarring [43, 44].

11β-HSD1 deletion was associated with greater collagen deposition and greater tissue myofibroblast numbers in the later phase of burn injury healing. This appeared to be due to greater differentiation of myofibroblasts but was associated with greater collagen deposition and increased tensile strength in healed wound tissues relative to WT mice. Barrier function of skin after wound healing is not a major clinical issue in contrast to scarring. Therefore, excessive scar tissue post burn is considered a critical problem from a patient perspective [45, 46]. These findings led us to explore whether selective targeting of synthetic glucocorticoids to cells expressing 11β-HSD1 could improve post-burn scarring. We demonstrated that application of custom-generated scaffolds containing either active or inactive glucocorticoids could reduce post-burn wound inflammation. This effect was however greater with the glucocorticoid that required activation by 11β-HSD1 than with its active counterpart [47]. Treatment with either glucocorticoid had significant effects to reduce the wound healing rate compared to the empty scaffold control; however, all wounds fully healed. At a later phase of wound healing, treatment with the inactive glucocorticoid, but not the active glucocorticoid, resulted in significantly reduced wound stiffness with no change in ultimate wound strength. These tissue properties indicated that application of 11β-HSD1-targeted glucocorticoid in its inactive form resulted in substantially better final scar properties than no glucocorticoid.

A greater *in vivo* effect of inactive substrates for 11β-HSD1 than their active counterparts has now been demonstrated in several situations. The effects of oral prednisolone on markers of bone formation were demonstrated to correlate most strongly with 11β-HSD1 activity rather than circulating levels of prednisolone, indicating that the effects on bone were more likely due to local 11β-HSD1-mediated reactivation of prednisolone from prednisone (which is generated *in vivo* from prednisolone predominantly in the kidney) [48]. More recently, mice with 11β-HSD1 KO were found to be resistant to many of the metabolic effects of treatment with corticosterone, the main active glucocorticoid in mice [49]. 11β-HSD1 knockout mice treated with glucocorticoids were also protected against bone loss and reduction in bone formation markers when treated with glucocorticoids, and an

additional study demonstrated a similar protection in terms of muscle wasting with glucocorticoids [50, 51]. These findings again indicate that tissue conversion of inactive to active glucocorticoids is a major contributor to the effect of these glucocorticoids rather than a direct effect of circulating active glucocorticoid [47, 52]. In the context of the current study it remains unclear why the inactive glucocorticoid treatments were superior to treatment with active glucocorticoid. It is possible that this could relate to subtle differences in the exposure to the two glucocorticoids. Although not significant statistically, there was a trend to a faster release of predisone in the early timepoints compared to that of prednisolone. This could alternatively be related to the apparent greater biological activity of inactive substrates of 11β-HSD1 compared to active substrates in cells expressing the enzyme described above. Additionally, it is possible that the multiple effects of active glucocorticoids on cell types not expressing 11β-HSD1 in the wound could lead to different outcomes. Given the dynamic and tissue-specific changes in 11β-HSD1 in response to burn injury, inactive glucocorticoids will only have effects in cells that express the enzyme, and these effects are likely to be greater in cells that express higher levels of activity. Active glucocorticoids cannot be targeted to just cells expressing 11β-HSD1 and will thus give similar exposure to all cells and tissues, regardless of 11β-HSD1 expression and the phase of wound healing.

This study has a number of limitations. The number of samples from burn patients is limited. The nature of burns in patients is inherently variable and difficult to standardize. The limited number of samples currently makes it difficult to determine whether additional factors influence 11β-HSD1 activity, e.g. patient age, gender, ethnicity and burn severity as assessed by TBSA affected by burn injury. A limitation of the murine studies is that some aspects of burn wound healing differ between humans and mice. Despite this, our burn injury model has been validated in several studies and replicates the same distinct but overlapping phases of burn injury healing seen in humans [31, 53, 54]. Whilst prednisone treatment has shown superior effects on reducing scar formation, other effects such as a delaying rate of wound healing could be considered detrimental to burn wounds. We were also unable to do functional testing of wound tissue on humans due to the destructive nature of these procedures. Future studies might examine coaxial electrospun scaffolds that encapsulate both an 11β-HSD1 inhibitor and prednisone, dynamically releasing an 11β-HSD1 inhibitor in the early phase of wound healing and inactive glucocorticoid in the later phase, potentially achieving both a faster wound healing rate and a reduction in scarring. In addition, future studies might also utilize non-invasive surrogate markers of mechanical properties, but it is unlikely that the comprehensive mechanical tests possible in rodents will be achievable in humans.

Conclusions

Overall these findings demonstrate an important role of 11β-HSD1 in both burn injury and scarring, and that controlled delivery of therapeutic agents, including an inactive glucocorticoid that could only be reactivated within skin cells expressing 11β-HSD1, is a novel approach to improve final scar characteristics. Moreover, through utilizing the 11β-HSD1 system, direct side-effects associated with overuse of topically applied active glucocorticoids is expected to be minimized. This information provides the logical basis for clinical trials of treatments designed to reduce the adverse features of healing in people with burn injury.

Abbreviations

Ct, Cycle threshold; H&E, Hematoxylin and eosin; HFP, Hexafluoro-2-propanol; 11β-HSD1, 11β-Hydroxysteroid dehydrogenase type 1 enzyme; IHC, Immunohistochemistry; IL-1β, Interleukin 1 beta; KO, knockout; PCNA, Proliferating cell nuclear antigen; PCL, Polycaprolactone; α-SMA, α-smooth muscle actin; TBSA: Total body surface area; TGF-β1, Transforming growth factor beta 1; TNF-α, Tumour necrosis factor alpha; COL1α1, Type I collagen; COL3α1, Type III collagen; WT, wild type.

Supplementary data

Supplementary data is available at *Burns & Trauma Journal* online.

Acknowledgements

KH-YT was supported by the Postgraduate Research Support Scheme from The Universityof Sydney. We are grateful to SN for mechanical property testing for scar tissues in the School of Chemical and Biomolecular Engineering and JT for developing the 11β-HSD1 KO mouse breeding colony.

Funding

This work was supported by National Health and Medical Research Council (NHMRC) fund (APP1101879), National Science Foundation of China (82172217) and ANZAC Research Institute near miss funding.

Authors' contributions

MSC, YW and KH-YT designed study. KH-YT, HS, RJP, SN, XD, XD, JJH, XW, WC, JC, QT, YW, ZL and ACIF contributed to experiments. KH-YT, MSC and YW analysed the data. KH-YT, MSC and YW wrote the paper. HS, RJP, SN, JC, PKM, and GGL assisted in the preparation of the manuscript. YW and MSC supervised the project.

Ethics approval

The animal breeding protocols and strategies have been approved by Sydney Local Health District Animal Welfare Committee (Protocol No 2013/074 and 2019/035). Animal studies were conducted under the approval of Sydney Local Health District Welfare Committee (Protocol No. 2018/020) under Australian National Health and Medical Research Council Guidelines for animal experimentation. Human studies were conducted following the ethical approval of Sydney Local Health District (Concord) Human Research Ethics

Committee (Protocol No. CH62/6/2014-139). All participants gave their written informed consent before study enrolment.

Conflicts of interest

None declared.

References

1. Jeschke MG, van Baar ME, Choudhry MA, Chung KK, Gibran NS, Logsetty S. Burn injury. *Nature Reviews Disease Primers*. 2020;6:1–25.
2. Evers LH, Bhavsar D, Mailänder P. The biology of burn injury. *Exp Dermatol*. 2010;19:777–83.
3. Ma L, Gan C, Huang Y, Wang Y, Luo G, Wu J. Comparative proteomic analysis of extracellular matrix proteins secreted by hypertrophic scar with normal skin fibroblasts. *Burns & Trauma*. 2014;2:2321–3868.130191.
4. Price K, Moiemen N, Nice L, Mathers J. Patient experience of scar assessment and the use of scar assessment tools during burns rehabilitation: a qualitative study. *Burns Trauma*. 2021;9:tkab005. https://doi.org/10.1093/burnst/tkab005.
5. Hosseini M, Brown J, Khosrotehrani K, Bayat A, Shafiee A. Skin biomechanics: a potential therapeutic intervention target to reduce scarring. *Burns Trauma*. 2022;10:tkac036. https://doi.org/10.1093/burnst/tkac036.
6. Xu X, Gu S, Huang X, Ren J, Gu Y, Wei C, *et al.* The role of macrophages in the formation of hypertrophic scars and keloids. *Burns Trauma*. 2020;8:tkaa006. https://doi.org/10.1093/burnst/tkaa006.
7. Xue M, Jackson CJ. Extracellular matrix reorganization during wound healing and its impact on abnormal scarring. *Adv Wound Care (New Rochelle)*. 2015;4:119–36.
8. Teot L, Otman S, Brancati A, Mittermayr R. Burn scar treatment. *Handbook of Burns*. 2012;55–67.
9. Robinson JK, Hanke CW, Siegel DM, Fratila A, Bhatia AC, Rohrer TE. *Surgery of the Skin E-Book: Procedural Dermatology*. Elsevier Health Sciences, 2014.
10. Stoughton RB. Steroid therapy in skin disorders. *J Am Med Assoc*. 1959;170:1311–5.
11. Hossain D. Steroid in the management of 2° superficial burn: a report. *Burns: journal of the International Society for Burn Injuries*. 2011;37:1460–1.
12. Jalali M, Bayat A. Current use of steroids in management of abnormal raised skin scars. *Surgeon*. 2007;5:175–80.
13. Ferguson J, Donald R, Weston T, Espiner E. Skin thickness in patients with acromegaly and Cushing's syndrome and response to treatment. *Clin Endocrinol*. 1983;18:347–53.
14. Stratakis CA. Skin manifestations of Cushing's syndrome. *Reviews in Endocrine and Metabolic Disorders*. 2016;17:283–6.
15. Tiganescu A, Walker EA, Hardy RS, Mayes AE, Stewart PM. Localization, age- and site-dependent expression, and regulation of 11β-hydroxysteroid dehydrogenase type 1 in skin. *J Invest Dermatol*. 2011;131:30–6.
16. Andrew R, Phillips DI, Walker BR. Obesity and gender influence cortisol secretion and metabolism in man. *The Journal of Clinical Endocrinology & Metabolism*. 1998;83:1806–6.
17. Hardy RS, Raza K, Cooper MS. Endogenous glucocorticoids in inflammation: contributions of systemic and local responses. *Swiss Med Wkly*. 2012;142:w13650. https://doi.org/10.4414/smw.2012.13650.
18. Hardy RS, Filer A, Cooper MS, Parsonage G, Raza K, Hardie DL, *et al.* Differential expression, function and response to inflammatory stimuli of 11β-hydroxysteroid dehydrogenase type 1 in human fibroblasts: a mechanism for tissue-specific regulation of inflammation. *Arthritis research & therapy*. 2006;8:R108. https://doi.org/10.1186/ar1993.
19. Terao M, Itoi S, Matsumura S, Yang L, Murota H, Katayama I. Local Glucocorticoid Activation by 11β-Hydroxysteroid Dehydrogenase 1 in Keratinocytes: The Role in Hapten-Induced Dermatitis. *Am J Pathol*. 2016;186:1499–510.
20. Ajjan RA, Hensor EMA, Del Galdo F, Shams K, Abbas A, Fairclough RJ, *et al.* Oral 11β-HSD1 inhibitor AZD4017 improves wound healing and skin integrity in adults with type 2 diabetes mellitus: a pilot randomized controlled trial. *Eur J Endocrinol*. 2022;186:441–55.
21. Terao M, Katayama I. Local cortisol/corticosterone activation in skin physiology and pathology. *J Dermatol Sci*. 2016;84:11–6.
22. Tiganescu A, Tahrani AA, Morgan SA, Otranto M, Desmoulière A, Abrahams L, *et al.* 11β-Hydroxysteroid dehydrogenase blockade prevents age-induced skin structure and function defects. *J Clin Invest*. 2013;123:3051-60.
23. Tiganescu A, Hupe M, Uchida Y, Mauro T, Elias PM, Holleran WM. Increased glucocorticoid activation during mouse skin wound healing. *J Endocrinol*. 2014;221:51–61.
24. Tiganescu A, Hupe M, Uchida Y, Mauro T, Elias PM, Holleran WM. Topical 11β-Hydroxysteroid Dehydrogenase Type 1 Inhibition Corrects Cutaneous Features of Systemic Glucocorticoid Excess in Female Mice. *Endocrinology*. 2018;159:547–56.
25. Terao M, Tani M, Itoi S, Yoshimura T, Hamasaki T, Murota H, *et al.* 11β-hydroxysteroid dehydrogenase 1 specific inhibitor increased dermal collagen content and promotes fibroblast proliferation. *PLoS One*. 2014;9:e93051. https://doi.org/10.1371/journal.pone.0093051.
26. Brazel CB, Simon JC, Tuckermann JP, Saalbach A. Inhibition of 11β-HSD1 Expression by Insulin in Skin: Impact for Diabetic Wound Healing. *J Clin Med*. 2020;9:3878.
27. Blackstone BN, Kim JY, McFarland KL, Sen CK, Supp DM, Bailey JK, *et al.* Scar formation following excisional and burn injuries in a red Duroc pig model. *Wound Repair Regen*. 2017;25:618–31.
28. Cohen J, Deans R, Dalley A, Lipman J, Roberts MS, Venkatesh B. Measurement of tissue cortisol levels in patients with severe burns: a preliminary investigation. *Crit Care*. 2009;13:R189. https://doi.org/10.1186/cc8184.
29. Semjonous NM, Sherlock M, Jeyasuria P, Parker KL, Walker EA, Stewart PM, *et al.* Hexose-6-phosphate dehydrogenase contributes to skeletal muscle homeostasis independent of 11β-hydroxysteroid dehydrogenase type 1. *Endocrinology*. 2011;152:93–102.
30. Zielinska AE, Fletcher RS, Sherlock M, Doig CL, Lavery GG. Cellular and genetic models of H6PDH and 11β-HSD1 function in skeletal muscle. *Cell Biochem Funct*. 2017;35:269–77.
31. Hew JJ, Parungao RJ, Shi H, Tsai KH, Kim S, Ma D, *et al.* Mouse models in burns research: Characterisation of the hypermetabolic response to burn injury. *Burns*. 2019;46:663–74.
32. Chen Y, Yu Q, Xu C-B. A convenient method for quantifying collagen fibers in atherosclerotic lesions by ImageJ software. *Int J Clin Exp Med*. 2017;10:14904–10.
33. Varghese F, Bukhari AB, Malhotra R, De A. IHC Profiler: an open source plugin for the quantitative evaluation and

automated scoring of immunohistochemistry images of human tissue samples. *PLoS One*. 2014;9:e96801. https://doi.org/10.1371/journal.pone.0096801.
34. Chong C, Wang Y, Fathi A, Parungao R, Maitz PK, Li Z. Skin wound repair: Results of a pre-clinical study to evaluate electrospun collagen–elastin–PCL scaffolds as dermal substitutes. *Burns*. 2019;45:1639–48.
35. Wei L-G, Chang H-I, Wang Y, Hsu S-H, Dai L-G, Fu K-Y, *et al.* A gelatin/collagen/polycaprolactone scaffold for skin regeneration. *PeerJ*. 2019;7:e6358. https://doi.org/10.7717/peerj.6358.
36. Chong C, Wang Y, Maitz PK, Simanainen U, Li Z. An electrospun scaffold loaded with anti-androgen receptor compound for accelerating wound healing. *Burns Trauma*. 2013;1:95–101. https://doi.org/10.4103/2321-3868.118935.
37. Kurakula M, Srinivas C, Kasturi N, Diwan PV. Formulation and evaluation of prednisolone proliposomal gel for effective topical pharmacotherapy. *Int J Pharm Sci Drug Res*. 2012;4:35–43.
38. Cerciello A, Auriemma G, Morello S, Aquino RP, Del Gaudio P, Russo P. Prednisolone delivery platforms: Capsules and beads combination for a right timing therapy. *PLoS One*. 2016;11:e0160266. https://doi.org/10.1371/journal.pone.0160266.
39. Mohammadi F, Samani SM, Tanideh N, Ahmadi F. Hybrid scaffolds of hyaluronic acid and collagen loaded with prednisolone: An interesting system for osteoarthritis. *Adv Pharm Bull*. 2018;8:11–19.
40. Lannutti J, Reneker D, Ma T, Tomasko D, Farson D. Electrospinning for tissue engineering scaffolds. *Mater Sci Eng C*. 2007;27:504–9.
41. Terao M, Murota H, Kimura A, Kato A, Ishikawa A, Igawa K, *et al.* 11β-Hydroxysteroid dehydrogenase-1 is a novel regulator of skin homeostasis and a candidate target for promoting tissue repair. *PLoS One*. 2011;6:e25039. https://doi.org/10.1371/journal.pone.0025039.
42. Emmerich J, van Koppen CJ, Burkhart JL, Engeli RT, Hu Q, Odermatt A, *et al.* Accelerated skin wound healing by selective 11β-Hydroxylase (CYP11B1) inhibitors. *Eur J Med Chem*. 2018;143:591–7.
43. Bullard KM, Longaker MT, Lorenz HP. Fetal Wound Healing: Current Biology. *World J Surg*. 2003;27:54–61.
44. Szpaderska AM, DiPietro LA. Inflammation in surgical wound healing: friend or foe? *Surgery*. 2005;137:571–3.
45. Bock O, Schmid-Ott G, Malewski P, Mrowietz U. Quality of life of patients with keloid and hypertrophic scarring. *Arch Dermatol Res*. 2006;297:433–8.
46. Robert R, Meyer W, Bishop S, Rosenberg L, Murphy L, Blakeney P. Disfiguring burn scars and adolescent self-esteem. *Burns*. 1999;25:581–5.
47. Slominski A, Zbytek B, Nikolakis G, Manna PR, Skobowiat C, Zmijewski M, *et al.* Steroidogenesis in the skin: implications for local immune functions. *J Steroid Biochem Mol Biol*. 2013;137:107–23.
48. Cooper MS, Blumsohn A, Goddard PE, Bartlett WA, Shackleton CH, Eastell R, *et al.* 11β-hydroxysteroid dehydrogenase type 1 activity predicts the effects of glucocorticoids on bone. *The Journal of Clinical Endocrinology & Metabolism*. 2003;88:3874–7.
49. Morgan SA, McCabe EL, Gathercole LL, Hassan-Smith ZK, Larner DP, Bujalska IJ, *et al.* 11β-HSD1 is the major regulator of the tissue-specific effects of circulating glucocorticoid excess. *Proc Natl Acad Sci*. 2014;111:E2482–91.
50. Martin CS, Cooper MS, Hardy RS. Endogenous Glucocorticoid Metabolism in Bone: Friend or Foe. *Front Endocrinol*. 2021;12:733611. https://doi.org/10.3389/fendo.2021.733611.
51. Webster JM, Sagmeister MS, Fenton CG, Seabright AP, Lai Y-C, Jones SW, *et al.* Global Deletion of 11β-HSD1 Prevents Muscle Wasting Associated with Glucocorticoid Therapy in Polyarthritis. *Int J Mol Sci*. 2021;22:7828. https://doi.org/10.3390/ijms22157828.
52. Vukelic S, Stojadinovic O, Pastar I, Rabach M, Krzyzanowska A, Lebrun E, *et al.* Cortisol synthesis in epidermis is induced by IL-1 and tissue injury. *J Biol Chem*. 2011;286:10265–75.
53. Abdullahi A, Amini-Nik S, Jeschke M. Animal models in burn research. *Cell Mol Life Sci*. 2014;71:3241–55.
54. Sullivan TP, Eaglstein WH, Davis SC, Mertz P. The pig as a model for human wound healing. *Wound Repair Regen*. 2001;9:66–76.